MEMS/NEMS based on mono-, nano-, and ultrananocrystalline diamond films

Anirudha V. Sumant, Orlando Auciello, Meiyong Liao, and Oliver A. Williams

Diamond, because of its unique physical, chemical, and electrical properties and the feasibility of growing it in thin-film form, is an ideal choice as a material for the fabrication of reliable, long endurance, microelectromechanical/nanoelectromechanical systems (MEMS/NEMS). However, various practical challenges, including wafer-scale thickness uniformity, CMOS compatibility, surface micromachining, and, more importantly, controlling the internal stress of the diamond films, make this material more challenging for MEMS engineers. Recent advances in the growth of diamond films using chemical vapor deposition have changed this landscape since most technical hurdles have been overcome, enabling a new era of diamond-based MEMS and NEMS development. This article discusses a few examples of MEMS and NEMS devices that have been fabricated using mono-, nano-, and ultrananocrystalline diamond films as well as their performance.

Introduction

Chemical vapor deposition (CVD) diamond film technology has experienced modest growth in the last two decades in terms of scientific and technological advances in the field, which has, ultimately, positively affected progress in diamond-based microelectromechanical/nanoelectromechanical systems (MEMS/NEMS). In the early 1990s, soon after realizing excellent mechanical, chemical, electrical, and optical properties of polycrystalline diamond films, which attracted attention from the MEMS community, the initial challenges ranged from mostly dealing with the rough microcrystalline morphology and developing surface micromachining processing techniques to the fabrication of basic MEMS structures (e.g., cantilever, bridges, comb-drive)[1,2] and characterization of mechanical properties such as Young's modulus, intrinsic stress, and fracture strength.

Soon after the introduction of nanocrystalline (NCD) and ultrananocrystalline diamond (UNCD) thin-film technology in the late 1990s, demonstrating mechanical and tribological properties close to that of single crystal diamond (SCD),[3] interest peaked in this area. Multiple groups worked from all over the world, leading to rapid progress in this field in recent years. Although in terms of optimizing residual stress (stress management), diamond thin-films are still not there yet as compared to silicon, it is now possible to control the residual stress in diamond films to a certain extent to fabricate "all diamond" moving MEMS devices with reasonable complexity.[4] Surface micromachining technology in diamond is now well matured, and advanced NEMS devices even in SCD have been demonstrated.[5,6]

Integration of diamond with piezoelectric materials such as PZT[7] and AlN[8] added another boost, enabling fabrication of high-performance piezoelectric-driven MEMS/NEMS. The first demonstration of complementary metal oxide semiconductor (CMOS) compatibility of UNCD[9] and thereafter fabrication of a radio frequency MEMS switch using UNCD as a dielectric layer driven by on-chip CMOS at wafer-scale[10] was a major step forward in diamond MEMS technology, paving the entry of diamond MEMS in communications electronics. Researchers are now successful in locating and manipulating electron spin associated with nitrogen-vacancy (NV) centers in diamond (substituted nitrogen atom in the diamond lattice paired with a nearest-neighbor vacancy) by applying external stimuli such as an electric field, magnetic field, microwave radiation or light, or a combination. This could be utilized to develop ultrasensitive NEMS sensors that can detect very weak magnetic fields (~few nano tesla)[11] useful for biomedical imaging.[12] The NV centers are also considered a basic

Anirudha V. Sumant, Argonne National Laboratory, IL, USA; sumant@anl.gov
Orlando Auciello, University of Texas at Dallas, USA; orlando.auciello@utdallas.edu
Meiyong Liao, National Institute for Materials Science, Japan; meiyong.liao@nims.go.jp
Oliver A. Williams, School of Physics and Astronomy, Cardiff University, UK; williamso@cf.ac.uk
DOI: 10.1557/mrs.2014.98

© 2014 Materials Research Society

building block to develop "quantum computers." This article focuses on a few specific examples covering important areas in diamond MEMS and NEMS, such as the fabrication of single crystal diamond NEMS switches, NCD-based NEMS devices, and CMOS compatible RF-MEMS switches that use UNCD as a dielectric.

Single crystal diamond NEMS switch

A NEMS switch is one of the potential solutions beyond CMOS. It is known that due to the scaling down of the feature size of CMOS, the power consumption is becoming a serious problem due to the high leakage currents in the semiconductors' transistors. NEMS offers the advantages of zero-leakage current and low-power consumption. However, current NEMS switches face various challenges. Silicon-based technologies suffer from problems of stiction, abrasion, and poor mechanical/tribological properties, leading to poor reliability of the NEMS devices. Carbon-based nanostructures such as carbon nanotubes are difficult to handle for practical device applications.[13]

Diamond is the ideal material to overcome the previously mentioned drawbacks due to its outstanding properties such as extremely high Young's modulus, the highest hardness, hydrophobic surface, low mass density, the highest thermal conductivity, high corrosion resistance to chemical attack by caustic chemicals,[14] and the feasibility of doping with boron atoms substituting carbon atoms in the lattice, or inserting nitrogen atoms in the grain boundaries of UNCD films[15] to produce electrically conductive diamond films. Kohn et al. fabricated micro-relays by using polycrystalline diamond.[2] MEMS actuators were fabricated using electrically conductive grain boundary-nitrogen-incorporated ultrananocrystalline diamond (N-UNCD) films with nitrogen atoms incorporated in the grain boundaries, providing excellent performance and reliability.[4]

For the case of SCD-based switches, a Type-Ib SCD substrate (contains up to 500 ppm of nitrogen impurities) implanted by high-energy carbon ions (180 keV) was utilized as the starting material for the batch fabrication of boron-doped SCD cantilevers/bridges and switches.[5,6] A homoepitaxial diamond layer doped with boron was grown on the implanted substrate by microwave plasma chemical vapor deposition (MPCVD) at a substrate temperature of 930°C. The high growth temperature facilitated the transformation of the damaged layer into graphite. An e-beam lithographic process was employed to define the cantilevers and bridge structures. An aluminum layer was utilized as a mask for reactive ion etching in an oxygen atmosphere. After that, the sample was etched in acid to fully relax the movable cantilever/bridge, while the other parts remained almost intact. After finishing the fabrication of the suspended nano-beams, e-beam evaporated Ti (50 nm)/Au (50 nm) layers were deposited on the patterned structures as electrical contacts. In principle, suspended nanoscale SCD structures in any shape could be produced by using the described process. SCD suspended cantilevers/bridges with various dimensions, including a width ranging from 100 to 400 nm and a length ranging from 2 to 16 µm, were fabricated.

The single crystal nature of the top diamond layer above the graphite was revealed by high-resolution transmission electron microscopy. A lateral device concept of diamond (conductive)-on-diamond (insulator) was proposed for the SCD NEMS switches, which offered a unique fabrication process different from those of conventional vertical structures based on the silicon substrate.[6] Various NEMS switches, such as two-terminal and three-terminal devices[6] were fabricated. The Type-Ib diamond substrate behaved as an excellent insulator, efficiently suppressing the leakage current in the devices.

Figure 1 shows a SCD cantilever (Figure 1a), bridge (Figure 1b), and the typical three-terminal (3T)-type NEMS switch (Figure 1c).[6] In the 3T switch, when a voltage is applied to the gate, dipolar attraction between the gate and source surface occurs. A simultaneously applied voltage to the drain generated a current in the circuit when the cantilever edge contacted the drain, as shown in Figure 1d. The ON and OFF states of the 3T-NEMS switch were well controlled by the gate voltage. The gate pull-in voltage ($V_{pull\text{-}in}$) was around 90 V for the 3T-NEMS switch, with dimensions of a cantilever

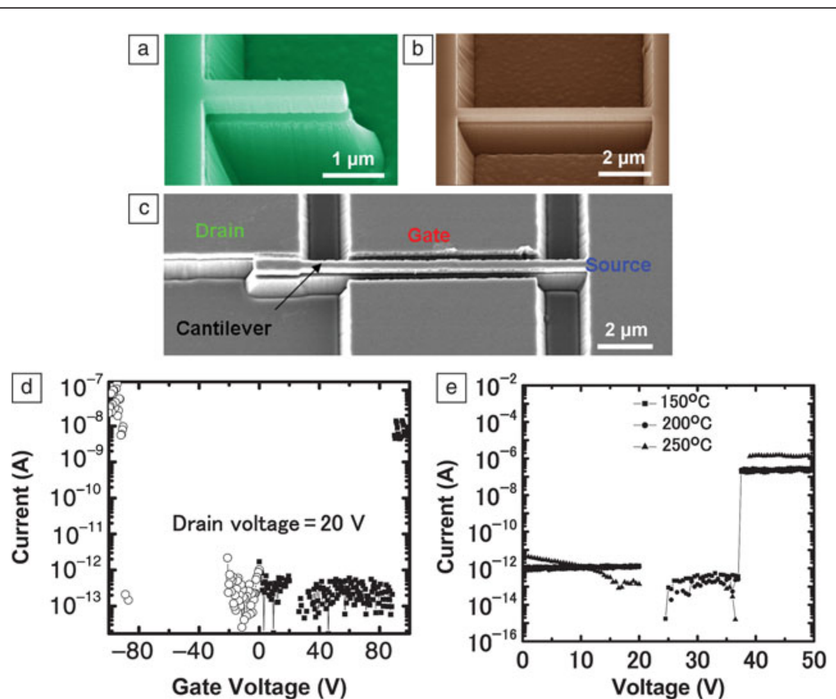

Figure 1. Scanning electron microscope images of single crystal diamond (a) cantilever, (b) bridge, and (c) 3T-nano-electromechanical systems switch; (d) current and gate voltage characteristics at a drain voltage of 20 V; (e) switching characteristics at elevated temperatures. Reproduced with permission from Reference 6. © 2010 Wiley.

length of 10 µm, a width of 400 nm, and a gate-source gap of 400 nm. Repeated switching did not change $V_{pull-in}$. The independence of $V_{pull-in}$ on the gate voltage polarity supported the electromechanical switching behavior. $V_{pull-in}$ could be reduced by properly designing the device structure such as by narrowing the cantilever width or by reducing the gap between the source and gate or lengthening the cantilever. For example, $V_{pull-in}$ is lower than 3 V for the cantilever with a length of 14 µm, a width of 200 nm, and a source-gate gap of 100 nm. Transient switching revealed that a long duration in the ON-state did not create a stiction problem even in air.

The NEMS switching devices exhibited an extremely low leakage current (<0.1 pA), which provided a high ON/OFF ratio of more than six orders of magnitude. The power consumption of the NEMS switch in the OFF state was lower than 1 pW, which was calculated from the gate voltage and source leakage current. The SCD NEMS switches exhibited high controllability and reproducibility. The 3T-NEMS switches also showed high reliability at elevated temperatures. No leakage current was found, and the $V_{pull-in}$ remained almost unchanged at least up to 523 K, as displayed in Figure 1e.[6]

The demonstration of all-SCD NEMS switches show that they not only overcome the existing problems of abrasion and stiction, but also show high controllability, high reproducibility, and high-temperature reliability, which gives them distinct advantage over silicon-based NEMS switches and, therefore, are promising for specialty applications.

NCD-based NEMS devices

The realization of thin NCD films with a Young's modulus equal to that of bulk diamond (1100 GPa)[16] has led to heightened research activity in high-frequency MEMS/NEMS both from a fundamental research point of view as well as for commercial applications. MEMS and NEMS resonators find application in areas as diverse as the filters and timing oscillators in wireless communications to the sensors in accelerometers and gyroscopes in navigation systems. GHz frequencies are readily achievable using NCD in paddle cantilever configurations, as shown in **Figure 2**(a–b).[17,18] This configuration is particularly impressive, exhibiting high-frequency-quality factor products (>10^{12}, 3x higher than for similar silicon structures) in such a simple structure. Recent surface acoustic wave devices fabricated from hybrid AlN/diamond structures have also shown resonant frequencies as high as 14 GHz.[19] Thus, S-band frequencies (2–4 GHz) and beyond are achievable with diamond technology, but it remains to be seen whether this technology will have any significant commercial impact.

There is also substantial interest in the fundamental science of materials and their integration into structures to fabricate MEMS and NEMS devices. For example, the dissipation (energy-loss) mechanisms of low-dimensional devices become highly nonlinear at low temperatures and are still not completely understood.[20,21] Another intriguing area is in the observation of macroscopic quantum mechanical effects. NEMS are ideal systems to study quantum mechanics because of their low dimensionality and associated mass, intrinsic low dissipation, and the ability to tune their resonant frequencies into the GHz range. The high resonant frequencies (GHz) of diamond cantilevers suggest that it should be possible to freeze out thermal fluctuations at low (mK) temperatures. The high Young's modulus and low density of diamond result in unrivalled sound wave velocities, and thus diamond cantilevers have substantially higher resonant frequencies than those made from other materials with the same dimensions. Therefore it should be possible to reach the standard quantum limit with diamond NEMS technologies by simply cooling a cantilever with resonant frequency in the GHz regime down to around 10 mK.

However, observing quantum fluctuations is significantly more involved. One suggestion has been to exploit the superconducting nature of boron-doped diamond in configurations such as a superconducting quantum interface device

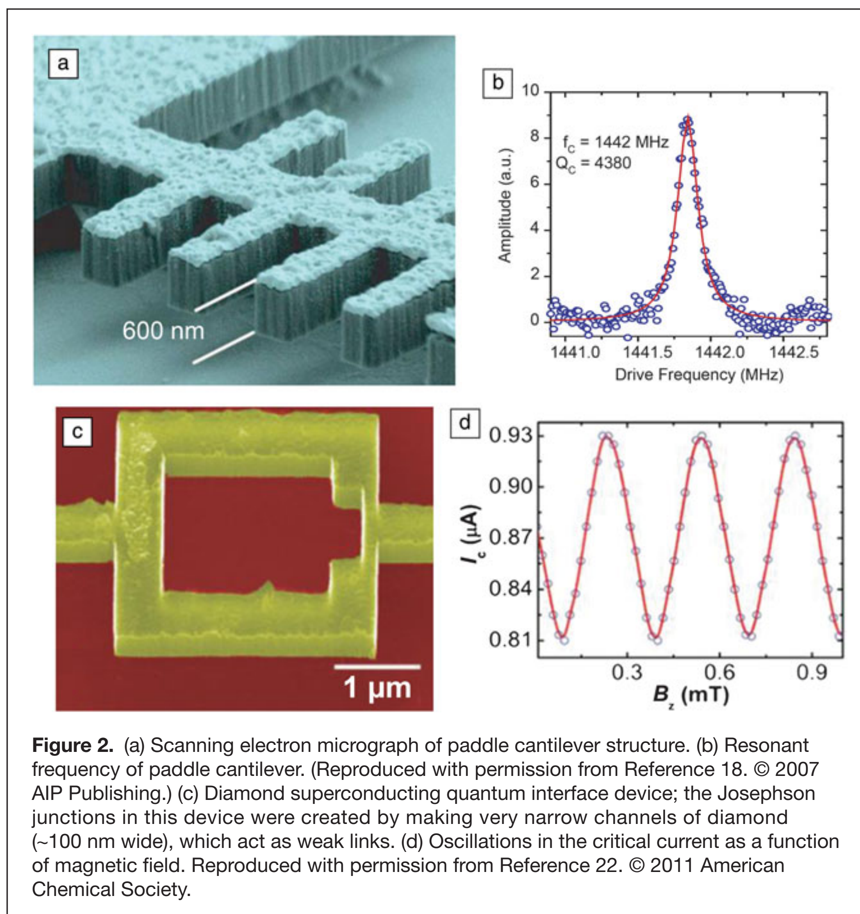

Figure 2. (a) Scanning electron micrograph of paddle cantilever structure. (b) Resonant frequency of paddle cantilever. (Reproduced with permission from Reference 18. © 2007 AIP Publishing.) (c) Diamond superconducting quantum interface device; the Josephson junctions in this device were created by making very narrow channels of diamond (~100 nm wide), which act as weak links. (d) Oscillations in the critical current as a function of magnetic field. Reproduced with permission from Reference 22. © 2011 American Chemical Society.

(SQUID).[22] A DC SQUID, shown in Figure 2c, consists of two Josephson junctions in a loop and exhibits periodic critical current oscillations as a function of the magnetic flux threading the loop with periodicity of the flux quantum, *h*/2e. This makes SQUIDs very sensitive to small changes in magnetic fields. Variations in the area of the SQUID will also be detectable, as they will result in a change in the magnetic flux penetrating the loop. By integrating a cantilever into one arm of the SQUID, it would be possible to detect its fluctuations, as small movements of the cantilever would modulate the area of the SQUID and thus the flux penetrating it. Thus, the quantum fluctuations of the cantilever would be observable as modulations in the SQUID's critical current (Figure 2d). Recently, it has been shown that diamond cantilevers can resonate in the superconducting state, and thus the detection of their motion within a DC SQUID is entirely feasible.[23]

CMOS compatible RF-MEMS switch using UNCD as a dielectric

The radio frequency (RF) MEMS switch (RF-MEMS) is one of the important components used in radar and mobile communication electronics.[24] RF switching can be accomplished using either solid-state junction devices based on III–V compound semiconductors (GaN, GaAs, InP) or standard silicon-based semiconductors such as SiC and SiGe. Alternatively, capacitive RF switches based on MEMS technology have become increasingly popular due to their low insertion loss, ultralow power consumption, and ultrahigh linearity.[25]

The RF-MEMS capacitive switch consists of a flexible metal membrane suspended over a lower electrode with an intermediate dielectric layer (**Figure 3**a). With application of sufficient electric field between the metal membrane and lower electrode, the metal membrane moves, thereby changing the capacitance to couple the RF signal to the desired path. When the applied field is released, the restoring force of the metal membrane is sufficient to disengage the metal membrane from contact to its normal position with an air gap that separates the upper membrane from the dielectric layer, thus disconnecting the RF signal.[26]

Despite the excellent RF performance of these switches, their acceptance in industry has been limited by a lack of long-term reliability. Some of the common failure modes in RF-MEMS capacitive switch include either dielectric breakdown after billions of cycles of operation, due to excessive charge build-up leading to switch failure, or sudden failure due to the stiction of the flexible metal membranes getting stuck to the dielectric layer under increased humidity conditions, leaving the switch in an inoperable condition. The most common materials used as a dielectric in an RF capacitive switch are silicon dioxide (SiO_2) and silicon nitride (Si_3N_4). Under continuous operation, charges get trapped and depleted over time, degrading the performance of the device until it fails. Studies have shown that oxide and nitride materials may charge in tens of seconds, but they discharge in hundreds of seconds, which leads to failure due to the membrane electrostatic-induced stiction onto the bottom electrode.[10,24,27]

UNCD thin films developed have been synthesized by the microwave MPCVD process using Ar/CH_4 gas chemistry that enables growth of UNCD films at low temperatures (~400°C)[9,28] compatible with the CMOS thermal budget processing. This enables integration of the RF-MEMS switches with CMOS devices, so the latter drive the switch.[10] The UNCD films are characterized by nanoscale grain size (2–5 nm)[3,6] and ultra-smooth surface roughness (5–7 nm).[3,28] More importantly, the unique grain boundary network structure of the UNCD films and thereby electronic properties of UNCD can be altered either by introducing nitrogen or hydrogen gas during the growth process. As a result, UNCD films can have either a semi-metallic or a leaky dielectric nature, respectively.[29] This leaky dielectric property of UNCD was further developed for a fast charging/discharging dielectric layer to cover the bottom electrode of the RF-MEMS switch[29,30] to replace the oxide or nitride dielectric that exhibits long discharging

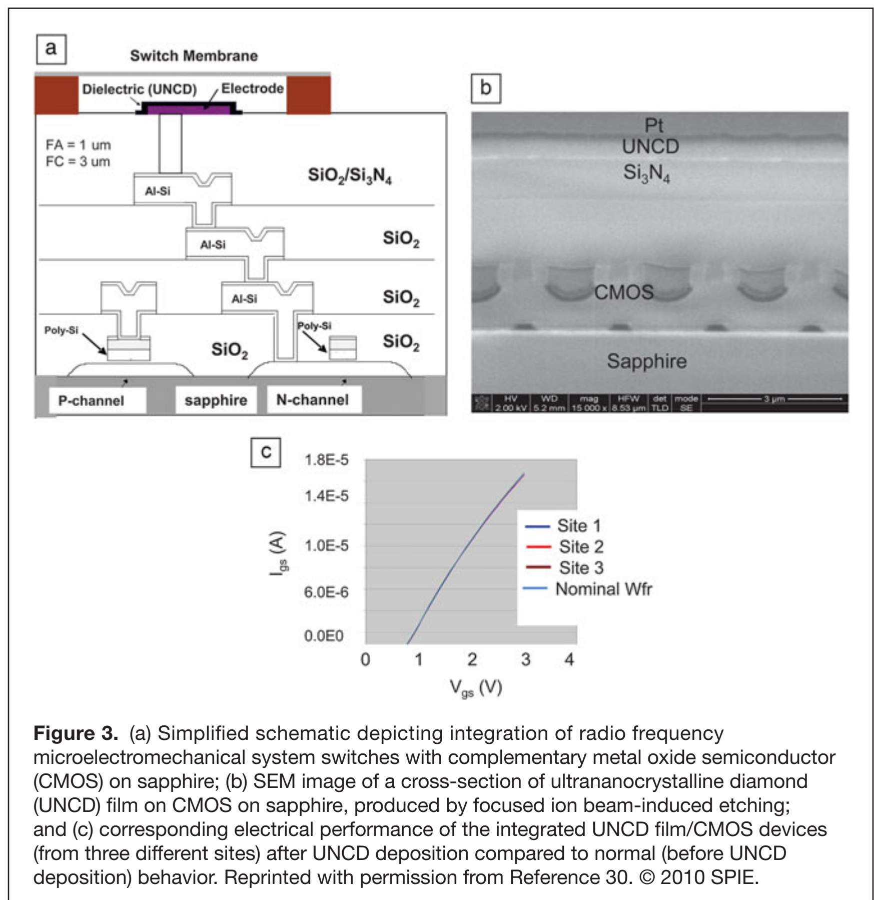

Figure 3. (a) Simplified schematic depicting integration of radio frequency microelectromechanical system switches with complementary metal oxide semiconductor (CMOS) on sapphire; (b) SEM image of a cross-section of ultrananocrystalline diamond (UNCD) film on CMOS on sapphire, produced by focused ion beam-induced etching; and (c) corresponding electrical performance of the integrated UNCD film/CMOS devices (from three different sites) after UNCD deposition compared to normal (before UNCD deposition) behavior. Reprinted with permission from Reference 30. © 2010 SPIE.

times, leading to switch failure. This work was the first demonstration of integration of a unique UNCD film technology with CMOS devices to implement monolithically integrated diamond-based MEMS/CMOS devices at the wafer scale level to enable a new device paradigm based on an on-chip CMOS-driven MEMS device.

The next step was to test CMOS compatibility with the UNCD films by directly growing UNCD films on sapphire-based CMOS-integrated circuits. Figure 3a shows a simplified schematic illustrating the integration of RF-MEMS switches with CMOS driving devices. Figure 3b shows a SEM picture of a cross-section, produced with a focused ion beam, of a CMOS device on sapphire wafer with a UNCD film grown on top at 400°C using MPCVD. The electrical performance of the UNCD-coated MOSFET device is shown in Figure 3c, with I–V characteristics plotted before and after UNCD film deposition. Both curves are superimposed, indicating that the CMOS device works to specification before and after growth of the UNCD films, thus demonstrating the great compatibility of the low-temperature UNCD film with CMOS technologies.

The first monolithically integrated UNCD RF-MEMS switches/SOS (silicon-on-sapphire)-CMOS devices (**Figure 4**) were fabricated following several microfabrication steps, including patterning, photolithography, deposition, reactive-ion etching (RIE), and chemical etching, described in more detail elsewhere.[10,29,30] Electrical measurements to test the RF performance of the RF-UNCD/MEMS switches revealed that they behave as typical MEMS capacitive switches.[10] For the shunt switch in the off-state, the insertion loss is very low (about 0.25 dB at 20 GHz). This insertion loss is slightly higher than the usual insertion loss of 0.15 dB observed in other RF-MEMS switches and is attributed to the less conductive tungsten metal used for the lower electrode, in comparison with Au electrodes used in other switches. When the switch is actuated, the isolation is set by the on-capacitance of the device. With 700 fF of on-capacitance measured for RF-UNCD/MEMS switches, the isolation at 20 GHz is very close to the theoretical value associated with a shunt 700 fF capacitor (7.7 dB). This switch operates more like a switched capacitor (45 fF–725 fF) than a high isolation switch at frequencies below 20 GHz.

Traditional RF-MEMS switches, using dielectric layers such as SiO_2 and Si_3N_4, typically exhibit bulk charging and discharging times of 10–100+ seconds. During switch operation, charges build up within and on top of the dielectric layer, resulting in a gradual change in the pull-in and release voltages until, ultimately, the switch fails. Considering that the main charging effect is thought to be concentrated in the bulk of the dielectric layer, the failure is characterized by the release voltage dropping to zero and the metallic membrane of the switch becoming stuck down on the dielectric layer. After failure, the switch requires a sufficiently long period of time to recover (in which the charges recombine) before the membrane is released. An additional effect that has not been carefully investigated is the hydrophilic nature (tendency to absorb water on the surface, resulting in interfacial adhesion) of the oxide or nitride layers and the metallic membrane, which may contribute to the stiction between the membrane and the oxide or nitride dielectric layers observed in the conventional RF-oxide/nitride MEMS switches.[24]

Systematic measurements of the response of RF-UNCD/MEMS switches revealed that these switches exhibit time constants that are five to six orders of magnitude quicker (about 100 μsec) than those of the switches with oxide or nitride layers (~10 to 100 seconds),[10] which is a substantial improvement. With these very short time constants (less than a millisecond after actuation), the switch temporarily stuck down after closing, but it recovers quickly after the switch bias is removed and is released as it should be in normal operation. The switch requires a very short time (~80 μsec) for the charge accumulated in the UNCD dielectric to dissipate through the dense network of UNCD grain boundaries, thus resulting in the switch release. The switch recovery time is not the typical 5–10 μs switching speed, but is dependent on the amount of charging that occurs during and after the switch closing. Thus, the time required for recovery and release is dependent on the time of the switch.

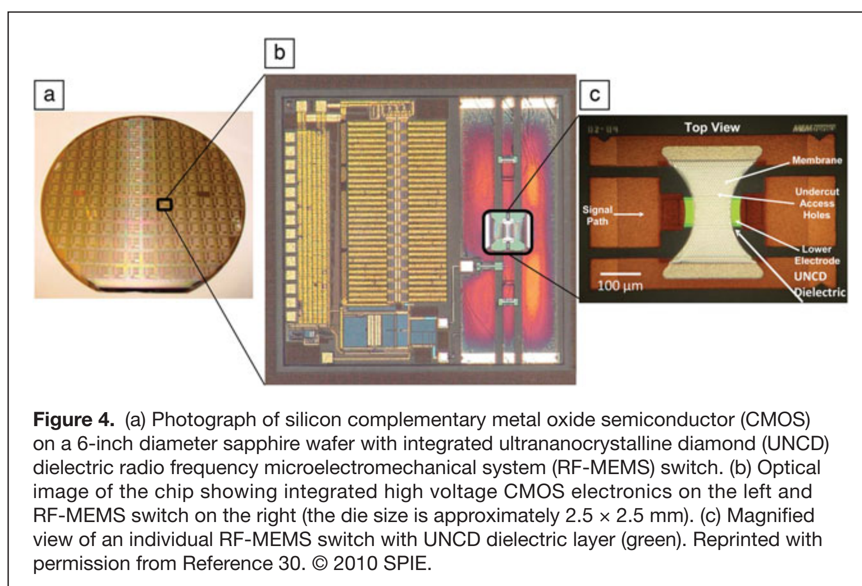

Figure 4. (a) Photograph of silicon complementary metal oxide semiconductor (CMOS) on a 6-inch diameter sapphire wafer with integrated ultrananocrystalline diamond (UNCD) dielectric radio frequency microelectromechanical system (RF-MEMS) switch. (b) Optical image of the chip showing integrated high voltage CMOS electronics on the left and RF-MEMS switch on the right (the die size is approximately 2.5 × 2.5 mm). (c) Magnified view of an individual RF-MEMS switch with UNCD dielectric layer (green). Reprinted with permission from Reference 30. © 2010 SPIE.

The reason for this uniquely different operation is that the charging and discharging time constants of the dielectric UNCD layer are very short. This is consistent with our basic understanding of the physics at work within the material. Charge carriers are concentrated at grain boundaries, and since the grains are nano-sized, they do not have far to travel to diffuse into or out of the UNCD dielectric layer. In essence, the switch pulls down and immediately charges to failure. However, when the applied voltage is removed, the charges leave

the dielectric very quickly through the large network of grain boundaries. It is easy to envision conditions under which the switch will recover from charging within a designated switching time interval (e.g., 50 μs). With this mode of operation, the switch will always recover fully from charging before the next switch operation ensues.

Lifetime tests for these switches have been carried out, and they survived for more than 12 billion cycles, demonstrating long-term reliability. The reliability of the RF-MEMS switch with the UNCD dielectric layer is enhanced due to the strong hydrophobic nature of the UNCD film surface, as demonstrated by extensive tests.[10,30] The results from electrical tests of the RF-MEMS switches with a UNCD dielectric demonstrate a new paradigm in RF-MEMS switch operation, one that potentially alleviates the scourge of dielectric charging as well as stiction problems, and therefore makes a strong case for diamond-based RF-MEMS to be utilized for commercial applications. In this respect, the RF-MEMS switch with UNCD dielectric is at the stage where a manufacturer of RF-MEMS switches for phase array antennas for radar and mobile communication devices should invest funds and efforts to take the technology from the prototyping stage to a real commercial product for realizing excellent potential benefits offered by this technology to defense sectors as well as in mobile communication devices.

Summary

Progress in CVD-diamond technology has directly resulted in the fabrication of advanced MEMS and NEMS devices based on diamond. These advances enabled fabrication of NEMS switches with ultra-low power consumption, high switching speed, and operation at high temperatures, however, more studies are needed to achieve similar performance on wafer-scale with polycrystalline diamond. Fundamental studies on understanding the mechanical dissipation in diamond cantilevers as well as electrical properties at very low temperature have led to designing ultrasensitive SQUID devices with the possibility of detecting a very weak magnetic field, promising for developing specialized sensors/detectors. The monolithic integration of UNCD films as a dielectric layer in an RF-MEMS switch with direct integration to CMOS demonstrates a paradigm shift in the operation of RF-MEMS switch technology and is a major step forward in developing CMOS compatible, CMOS driven diamond MEMS for efficient radar and mobile communications.

Acknowledgments

A.V.S. and O.A. would like to acknowledge funding supported by DARPA under contracts MIPR 06-W238, and by the US Department of Energy, Office of Science, Office of Basic Energy Sciences-Materials Science, under Contract No. DE-AC02–06CH11357. Use of the Center for Nanoscale Materials was supported by the US Department of Energy, Office of Science, and Office of Basic Energy Sciences under Contract No. DE-AC02–06CH11357. O.A. would like to acknowledge support from UTD through the Endowed Chair Professor initiation. O.W. would like to acknowledge Marie Curie Actions for his Intra-European Fellowship.

References

1. A.R. Krauss, O. Auciello, D.M. Gruen, A. Jayatissa, A.V. Sumant, J. Tucek, D.C. Mancini, N. Moldovan, A. Erdemir, D. Ersoy, M.N. Gardos, H.G. Busmann, E.M. Meyer, M.Q. Ding, *Diam. Relat. Mater.* **10**, 1952 (2001).
2. E. Kohn, P. Gluche, M. Adamschik, *Diam. Relat. Mater.* **8**, 934 (1999).
3. J.E. Butler, A.V. Sumant, *Chem. Vap. Depos.* **14** (7–8), 145 (2008).
4. F. Buja, A.V. Sumant, W.M. van Spengen, *Solid-State Sensors, Actuators and Microsystems* 2349 (2013), doi: 10.1109/Transducers.2013.6627277.
5. M.Y. Liao, C. Li, S. Hishita, Y. Koide, *J. Micromech. Microeng.* **20**, 085002 (2010).
6. M.Y. Liao, S. Hishita, E. Watanabe, S. Koizumi, Y. Koide, *Adv. Mater.* **22**, 5393 (2010).
7. S. Sudarsan, J. Hiller, B. Kabius, O. Auciello, *Appl. Phys. Lett.* **90**, 134101 (2007).
8. M. Zalazar, P. Gurman, J. Park, D. Kim, S. Hong, L. Stan, R. Divan, D. Czaplewski, O. Auciello, *Appl. Phys. Lett.* **102**, 104101 (2013).
9. A.V. Sumant, O. Auciello, H.-C. Yuan, Z. Ma, R.W. Carpick, D.C. Mancini, *Proc. SPIE Int. Soc. Opt. Eng.* **7317**, 731817 (2009).
10. C. Goldsmith, A. Sumant, O. Auciello, J. Carlisle, H. Zeng, J.C.M. Hwang, C. Palego, W. Wang, R. Carpick, V. Adiga, A. Datta, C. Gudeman, S. O'Brien, S. Sampath, *IEEE Int. Microw. Symp. Dig.* 1246 (2010).
11. J.R. Maze, P.L. Stanwix, J.S. Hodges, S. Hong, J.M. Taylor, P. Cappellaro, L. Jiang, M.V.G. Dutt, E. Togan, A.S. Zibrov, A. Yacoby, R.L. Walsworth, M.D. Lukin, *Nature* **455**, 644 (2008).
12. J.M. Taylor, P. Cappellaro, L. Childress, L. Jiang, D. Budker, P.R. Hemmer, A. Yacoby, R. Walsworth, M.D. Lukin, *Nat. Phys.* **4**, 810 (2008).
13. S.W. Lee, D.S. Lee, R.E. Morjan, S.H. Jang, M. Sveningsson, O.A. Nerushev, Y.W. Park, E.B. Campbell, *Nano Lett.* **4**, 2027 (2004).
14. M. Adamschik, J. Kusterer, P. Schmid, K.B. Schad, D. Grobe, E. Kohn, *Diam. Relat. Mater.* **11**, 672 (2002).
15. S. Battacharyya, O. Auciello, J. Birrell, J.A. Carlisle, L.A. Curtiss, A.N. Goyete, D.M. Gruen, A.R. Krauss, J. Schlueter, A.V. Sumant, P. Zapol, *Appl. Phys. Lett.* **79** (10), 1441 (2001).
16. O.A. Williams, A. Kriele, J. Hees, M. Wolfer, W. Muller-Sebert, C.E. Nebel, *Chem. Phys. Lett.* **495**, 84 (2010).
17. J. Wang, J.E. Butler, T. Feygelson, C.T.C. Nguyen, 17th IEEE International Conference on Micro Electro Mechanical Systems, *Technical Digest.* 641 (2004).
18. A. Gaidarzhy, M. Imboden, P. Mohanty, J. Rankin, B.W. Sheldon, *Appl. Phys. Lett.* **91**, 203503 (2007).
19. J.G. Rodriguez-Madrid, G.F. Iriarte, J. Pedros, O.A. Williams, D. Brink, F. Calle, *IEEE Electron Device Lett.* **33**, 495 (2012).
20. M. Imboden, O. Williams, P. Mohanty, *Appl. Phys. Lett.* **102**, 103502 (2013).
21. M. Imboden, O.A. Williams, P. Mohanty, *Nano Lett.* **13**, 4014 (2013).
22. S. Mandal, T. Bautze, O.A. Williams, C. Naud, E. Bustarret, F. Omnes, P. Rodiere, T. Meunier, C. Baeuerle, L. Saminadayar, *ACS Nano* **5**, 7144 (2011).
23. T. Bautze, S. Mandal, O.A. Williams, P. Rodière, T. Meunier, C. Bäuerle, *Carbon* **72**, 100 (2014).
24. G.M. Rebeiz, *RF MEMS, Theory, Design and Technology* (Wiley, NY, 2003).
25. Z.J. Yao, S. Chen, S. Eshelman, D. Denniston, C. Goldsmith, *J. Microelectromech. Syst.* **8** (2), 129 (1999).
26. C.L. Goldsmith, Z. Yao, S. Eshelman, D. Denniston, *IEEE Microwave and Guided Wave Lett.* **8** (8), 269 (1998).
27. O. Auciello, S. Pacheco, A.V. Sumant, C. Gudeman, S. Sampath, A. Datta, R.W. Carpick, V.P. Adiga, P. Zurcher, Z. Ma, H.C. Yuan, J.A. Carlisle, B. Kabius, J. Hiller, *IEEE Microwave Mag.* **8**, 61 (2008).
28. A.V. Sumant, O. Auciello, R.W. Carpick, S. Srinivasan, J.E. Butler, *MRS Bull.* **35**, 281 (2010).
29. A.V. Sumant, O. Auciello, D. Mancini, US Patent 8,354,290 B2 (2013).
30. O. Auciello, A.V. Sumant, C. Goldsmith, S. O'Brien, S. Sampath, C. Gudeman, W. Wang, J.C.M. Hwang, J. Swonger, J.A. Carlisle, S. Balachandran, D.C. Mancini, *Proc. in SPIE* **7679**, 9 (2010).

www.mrs.org